Astronomy & Astrophysics manuscript no.
(will be inserted by hand later)

Unusual profile variations in pulsar PSR J1022+1001 – Evidence for magnetospheric "return currents"?

R. Ramachandran[1,2] and M. Kramer[3]

[1] Department of Astronomy, University of California at Berkeley, Berkeley, CA 94720, USA
[2] Stichting ASTRON, PO Box 2, 7990 AA Dwingeloo, The Netherlands
[3] Jodrell Bank Observatory, University of Manchester, Macclesfield, Chesire SK11 9DL, UK

Received 31-03-03 / Accepted 01-07-03

Abstract. We report a detailed multi-frequency study of significant instabilities observed in the average pulse profile of the 16-millisecond pulsar PSR J1022+1001. These unusual profile variations which are seen as a function of time and of radio frequency are clearly different from classical profile mode-changing. We also note discrete jumps in the polarisation position angle curve of this pulsar which are remarkably coincident with the unstable profile component. We propose that these jumps, as well as the instability of the pulse profile, are due to magnetospheric return currents. This would allow us to measure the basic properties of the magnetospheric plasma for the very first time.

Key words. Stars: neutron; pulsars: PSR J1022+1001; Stars: emission; Plasmas

1. Introduction

The great success of pulsar timing and its numerous exciting applications, e.g. in the study of gravitational physics (e.g. Taylor 1994), is often only possible due to the high precision which is obtained during pulse time-of-arrival (TOA) measurements. The procedure for obtaining TOAs involves cross-correlating the observed time-tagged pulse profile with a high signal-to-noise standard pulse profile (*template*) that is typically generated iteratively using earlier observations. The implicit assumption is made that the average pulse profile remains stable over a long time and small frequency ranges. This assumption is usually well justified. In particular, a few minutes of observation for millisecond pulsars (MSPs) leads to the integration of several tens of thousand of single pulses, that is far beyond the usual time scale of a few hundred to thousand pulses necessary to obtain a stable pulse profile (e.g. Helfand et al. 1975). Until recently, only two fast rotating pulsars were known to exhibit slow profile changes. These were PSR B1913+16 (Weisberg et al. 1989, Kramer 1998) and PSR B1534+12 (Arzoumanian 1995, Stairs et al. 2000) which both show profile changes on secular time scales due to gravitational spin-orbit coupling.

This understanding that average profiles of MSPs are perfectly stable, changed considerably with the observations of the 16-ms pulsar PSR J1022+1001 (Camilo 1994) made with the Effelsberg radio telescope (Kramer et al. 1999a, hereafter K99). This pulsar in a 7.8-d binary orbit with a heavy CO white dwarf exhibits a characteristic double-peaked average profile. The reported pulse shape changes are most easily recognized by an alteration of the ratio of the two component amplitudes. This, of course, results in large TOA variations when the pulsar is timed with a single standard template. Using an *adaptive* template however, K99 were able to obtain a timing accuracy that is comparable to other, ordinary millisecond pulsars. The detailed analysis by K99 furthermore showed that, out of the two prominent components, only the leading, weakly polarised component seems to undergo changes in intensity and structure, while the trailing, highly polarised component remained stable, and arrived "on time".

While this different behaviour of the two components points to an effect intrinsic to the pulsar magnetosphere, K99 also looked for possible relationships of the profile changes to other effects, such as time of day, parallactic angle, or even seasonal changes. None of these, however, shows any correlation with the profile changes, and in fact, a typical timescale for the pulse shape variations could not be identified. An explanation for this appears to come from a totally unexpected result obtained by K99.

Observations by K99 revealed that PSR J1022+1001 does not only show profile variations as a function of time, but also on a narrow range of radio frequency! As K99 measured, the average profile at 1400 MHz changes its shape on a typical frequency scale of about 8 MHz. Moreover, the modulation of the leading component resembles closely to what one expect from interstellar scin-

Table 1. List of observations made. The five columns give the date of observation, centre frequency, bandwidth, number of frequency channels and the effective sampling interval, respectively.

Date (dd:mm:yy)	$\nu_{\rm centre}$ (MHz)	$\Delta\nu$ (MHz)	$\mathbf{N}_{\rm chn}$	$\Delta t_{\rm eff}$ (μs)
18-03-01	1380	80	512	51.4
08-03-01	840	80	512	56.0
08-03-01	328	10	512	113
08-03-01	382	10	256	119
22-03-01	1380	80	512	51.4
22-03-01	328	10	512	113
22-03-01	382	10	256	119
22-03-01	840	80	512	56.0
05-04-01	840	80	512	56.0
05-04-01	1380	80	512	51.4
05-04-01	328	10	512	113
05-04-01	382	10	256	119

tillation, where the bright "scintils" correspond to the flaring up of the leading component. While this variation of the average profile as a function of narrow frequency range points again to processes in the pulsar magnetosphere, it indeed explains why no typical time scales for the profile changes have been discovered yet; depending on the temporal intensity maximum within the observing band, determined by the ordinary interstellar scintillation, and the actual profile-frequency pattern, different pulse profiles can be observed with different timescales.

Meanwhile, profile variations have also been reported for the millisecond pulsars PSR B1821−24 (Backer & Sallmen 1997), and PSR J1730−2304 (K99), while significant changes in the polarisation states have been identified for PSR J2145−0750 (Xilouris et al. 1998, Sallmen 1998, Stairs et al. 1999). None of these sources has been studied carefully for profile changes over a narrow frequency range, since peak flux densities are usually smaller than for PSR J1022+1001.

In this work we concentrate on PSR J1022+1001 in order to study the extraordinary narrow frequency band profile variation in more detail. We report observations of this pulsar made with the Westerbork Synthesis Radio Telescope (WSRT) at four different centre frequencies, i.e. at 1380, 840, 382 and 328 MHz. These observations were motivated by the work of Lyutikov & Parikh (2000) and Lyutikov (2001) who picked up the comments made by K99 and suggested that the profile variations could indeed be caused by scattering of emission near the light cylinder. In this case, it is obviously important to study the narrow-band profile changes at various radio frequencies.

We also propose in this paper that the observed polarisation properties of this pulsar are closely related to the instabilities that we see in one of the components. As we will demonstrate, there is a striking similarity between the observed average polarisation position angle as a function of pulse longitude and the predictions of Hibschman & Arons (2001), who discuss the possible effect of aberration and polar cap current flows on the observed polarisation position angle curve. If this is true, then our results become the first ever evidence for return currents in the pulsar magnetosphere.

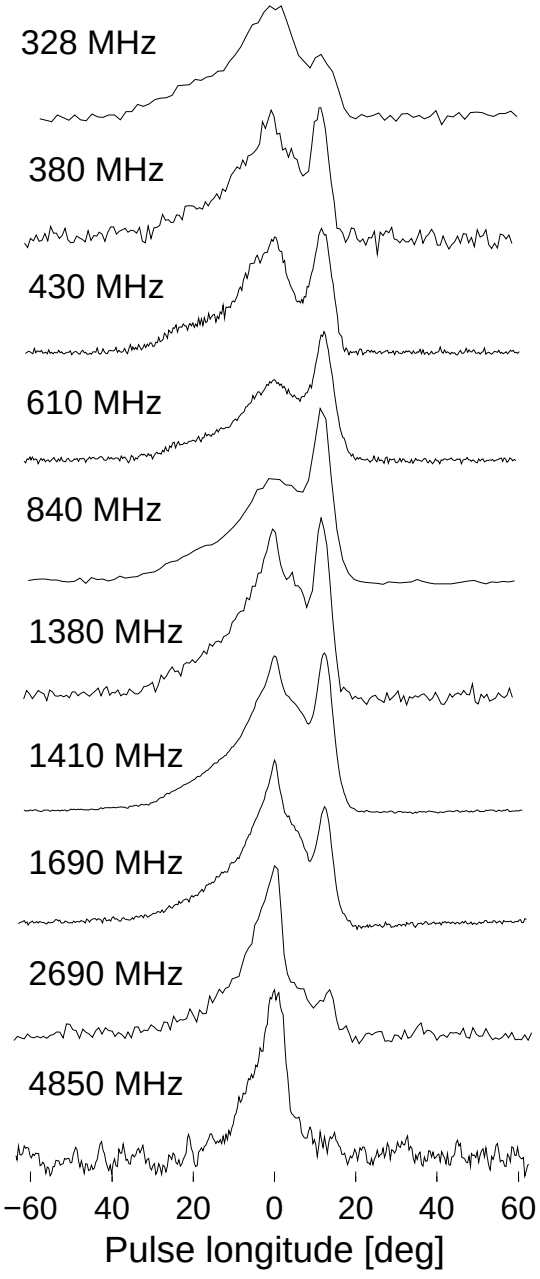

Fig. 1. Long term average profiles of J1022+1001 at various radio frequencies. Profiles at 328, 382, 840 and 1380 MHz are from our present observations. All the other profiles have been taken from Kramer et al. (1999b) and references therein. Bandwidths of these observations are (from 328 MHz to 4850 MHz) 10, 10, 10, 10, 80, 80, 40, 40, 80 and 112 MHz, respectively.

After describing our observing set-up and procedures (Sect. 2), we describe the observed characteristics of pulse profile variation (Sect. 3 – 4). This includes discussion on their long term and short term behaviour, and their possible relation to classical "mode-changing". In Sect. 5, we describe the observed polarisation properties of this pulsar and possible explanations. This is followed by discussion and conclusions from this investiation.

2. Observations

Observations were made in March to April 2001 with the pulsar backend, `PuMa`, at the WSRT. The WSRT is an east-west array, with fourteen equatorially mounted 25-m dishes. We have chosen this telescope for its frequency agility combined with a powerful state-of-the-art pulsar data acquisition system, and in particular we have chosen it for its equatorial mount.

Even if only Stokes-I (total intensity) is recorded, there is in principle a chance that severe polarisation cross-coupling effects between signals from the two dipoles can affect the strength and shape of the pulse profile. For instance, cross coupling can reduce the observed total power of a randomly polarised signal by a certain fraction, independent of the absolute orientation of the dipoles to the plane of the sky. For a completely linearly polarised signal, the observed signal strength can vary as a function of the absolute dipole orientation with respect to the direction of linear polarisation of the signal. When a partially linearly polarised source drifts in the plane of the sky during the observation, the direction of linear polarisation of the source signal incident on the antenna feeds changes for alt-azimuth mounted telescopes. For a telescope system with severe cross-coupling errors, this may introduce some time-dependence of the observed profile structure, as a function of parallactic angle. As K99 demonstrate, this dependence is not observed in the previous Effelsberg observations of PSR J1022+1001, but cannot be fully excluded for the Arecibo observations also studied by K99. Therefore, in order to exclude any such instrumental effect, we choose to observe this pulsar with the WSRT. With the WSRT being an equatorially mounted telescope, the position angle of a linearly polarised astronomical source remains constant with respect to the orientation of the dipole as the source moves in the plane of the sky during the observations. Any aforementioned effect with the potential to alter the observed shape of the profile can therefore be excluded.

We used the WSRT at four different frequencies as detailed in Table 1. For each observation, the delays between the dishes were compensated and the signals were added "in phase" to construct an equivalent 94-m single dish having an aperture sensitivity of about 1.2 K Jy^{-1}. The frontends in all used bands consisted of two orthogonal linear dipoles. In the WSRT signal pipeline, the maximum allowed bandwidth at any given band per polarisation channel is 80 MHz. In the intermediate frequency signal path, this 80 MHz is divided into eight 10 MHz bands (whose individual centre frequencies can be configured independently within the allowed frequency range of the front end). For our 1380 MHz and 840 MHz observations, we chose a contiguous frequency band of 1340–1420 MHz and 800–880 MHz, respectively.

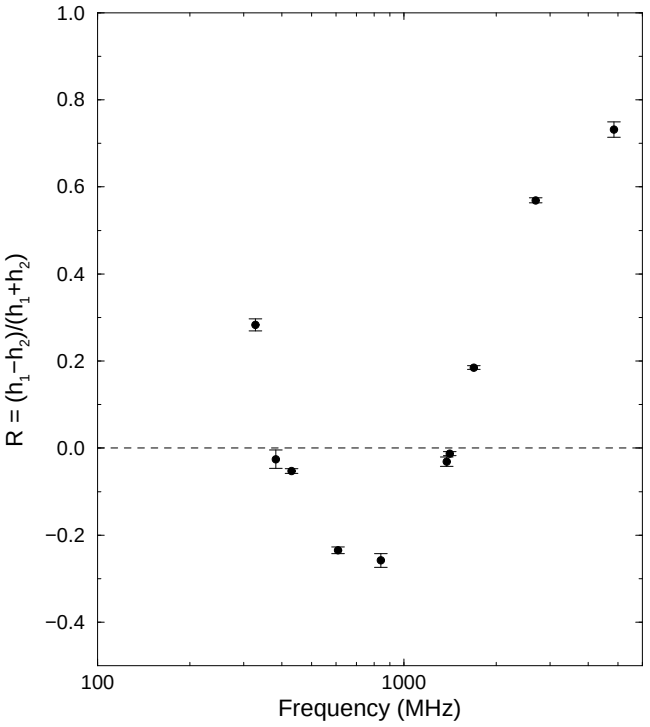

Fig. 2. Normalised component amplitude ratio R as a function of radio frequency. A value of $0 < R \leq +1$ indicates a dominance of the leading component, while for $-1 \leq R < 0$ the trailing component is stronger. There is a strikingly systematic behaviour, with a minimum at a frequency of about 800 MHz.

Signals from each of the 10 MHz bands were Nyquist-sampled and Fourier transformed to synthesize a filterbank of some specified number of spectral channels. Finally, after some averaging, the 2-bit (4 level) power samples were recorded in all the frequency channels. The final effective sampling interval in each observation is given in Table 1.

We compensated for the interstellar dispersion in each of these observed data sequence by assuming a dispersion measure of 10.246 pc cm^{-3} (K99).

3. Average profile evolution over large frequency range

Average pulse profiles of pulsars are known to exhibit systematic changes as a function of radio frequency. There are a number of extensive studies in the literature which concentrate on this very issue (e.g. Rankin 1983; Hankins & Rickett 1986; Lyne & Manchester 1988, Kramer et al. 1994; Moffett & Hankins 1996; Mitra & Rankin 2002). A typical profile evolution would exhibit a narrowing of

the pulse width at higher frequencies, while at the same time the outer profile components become stronger relative to the central components. The most common understanding of frequency-dependent systematic change is on the basis of the so called *radius-to-frequency* mapping where radio emission of higher frequencies are emitted closer to the neutron star than that of lower frequencies (e.g. Ruderman & Sutherland 1975). Mitra & Rankin (2002) give a recent complete summary of our understanding of these effects.

Kramer et al. (1999b) showed that this picture of "typical" profile evolution cannot be applied to millisecond pulsars. In fact, they pointed out that in most cases, profile evolution with frequency is minimal for millisecond pulsars and that the profile width hardly ever changes. They argue that the small size of a millisecond pulsar magnetosphere does not allow a large stratification in emission height and that in this case, the emission virtually comes from a single location in the magnetosphere.

One notable exception to this distinctive millisecond pulsar behaviour is again PSR J1022+1001, whose magnetosphere is however considerably larger due to its relatively long spin-period of 16 ms. Kramer et al. (1999b) presented a number of multi-frequency profiles for this pulsar, showing a remarkable frequency evolution. We improve their summary here with additional profiles obtained from our observations which are aligned by eye (see Fig. 1).

The profiles shown are grand averages over all available observing time and bandwidth (80 MHz in our case), which finally averages out the effects which we will discuss in more detail in the following section. Nevertheless, the profile evolution of this set of the grand averages of PSR J1022+1002 is quite exceptional, and not easy to explain.

At 328 MHz, the leading component is stronger. However, both components stay almost equal in strength at 380 MHz and 430 MHz, after which the trailing component becomes stronger. At 840 MHz the height of the leading component is only about 60% of the trailing component. Above this frequency, the relative strength of the leading component increases, and at the highest frequency (4848 MHz), the trailing component is almost non-existent though still detectable. This unusual behaviour is summarised very nicely in Fig. 2, where we have plotted a function of the component amplitudes h_1 (leading) and h_2 (trailing), defined as $R \equiv (h_1 - h_2)/(h_1 + h_2)$. R has values between $+1$ and -1 depending on the relative strength of the leading and trailing component. The plot of R looks strikingly systematic in its behaviour. Curiously, there is a minimum at radio frequency of about 800 MHz. This strange behaviour of R with frequency clearly shows that the two components exhibit entirely different frequency scalings. The profile is hardly evolving over the frequency interval from 600 to 800 MHz and at very high frequencies. The profile evolves fastest at frequencies around 500 MHz, 1400 MHz and very low frequencies.

This frequency evolution is unusual when compared to both normal pulsars (e.g. Mitra & Rankin 2002) and millisecond pulsars (Kramer et al. 1999b). It is obviously impossible to describe the flux density spectrum of both components by a simple power law across all frequencies. These results confirm the unusual spectral properties of both components which are superposed on the profile variations at a single frequency.

4. Profile Instabilities

As K99 show, the leading component of the profile shows instabilities, although the trailing component is very stable. In the following sections, we study this in detail, both as a function of radio frequency and time.

4.1. Narrow-band variations

In order to study the profile variations over a narrow frequency range, we folded the de-dispersed time series in each frequency channel at the period of the pulsar to generate average pulse profiles. An average pulse profile was produced for every specified interval of time (typically 8 min) in each frequency channel. Each time interval was long enough to have several tens of thousands of rotation periods, so that we can expect that fluctuations of the individual pulses as known for normal pulsars (Helfand et al. 1975) are averaged out.

Unfortunately, the pulsar was very weak during our observations at 328 MHz and 382 MHz. However, our observations at 840 MHz and 1380 MHz were strong enough for us to investigate the phenomenon that we will describe below.

Fig. 3 shows the contour plot using the 1380 MHz data set of average pulse profiles as a function of radio frequency. The two vertical trails of contours correspond to the two components of the average pulse profile. This plot corresponds to a time interval of 8 min ($\sim$ 30,000 individual pulses). Although the original observation had 512 frequency channels across the 80 MHz bandwidth, after de-dispersion, due to signal-to-noise ratio considerations, we have added 32 adjacent channels, so that the band is represented by only 16 channels. For clarity, the average pulse profiles in all the frequency channels are normalised in such a way that the height of the stable trailing component is unity (right-side vertical contour strip). However, the leading component, as the contours (as well as the five inserted plots) show, is unstable. The five inserted average profiles (from bottom to top) correspond to frequency channels 1, 5, 9, 13 and 16, respectively. Contour levels have been plotted in steps of root mean square error (Eqn. 1). The observed profile variations are perfectly consistent with the results presented by K99 using a different telescope with different polarisation feeds, different hardware, and in particular with a different telescope mount.

It is important to appreciate that this instability of the leading component is not due to interstellar scintillation, for it affects both the components equally. Since we have normalised the height of the trailing component to unity, the relative variation seen in the leading component must

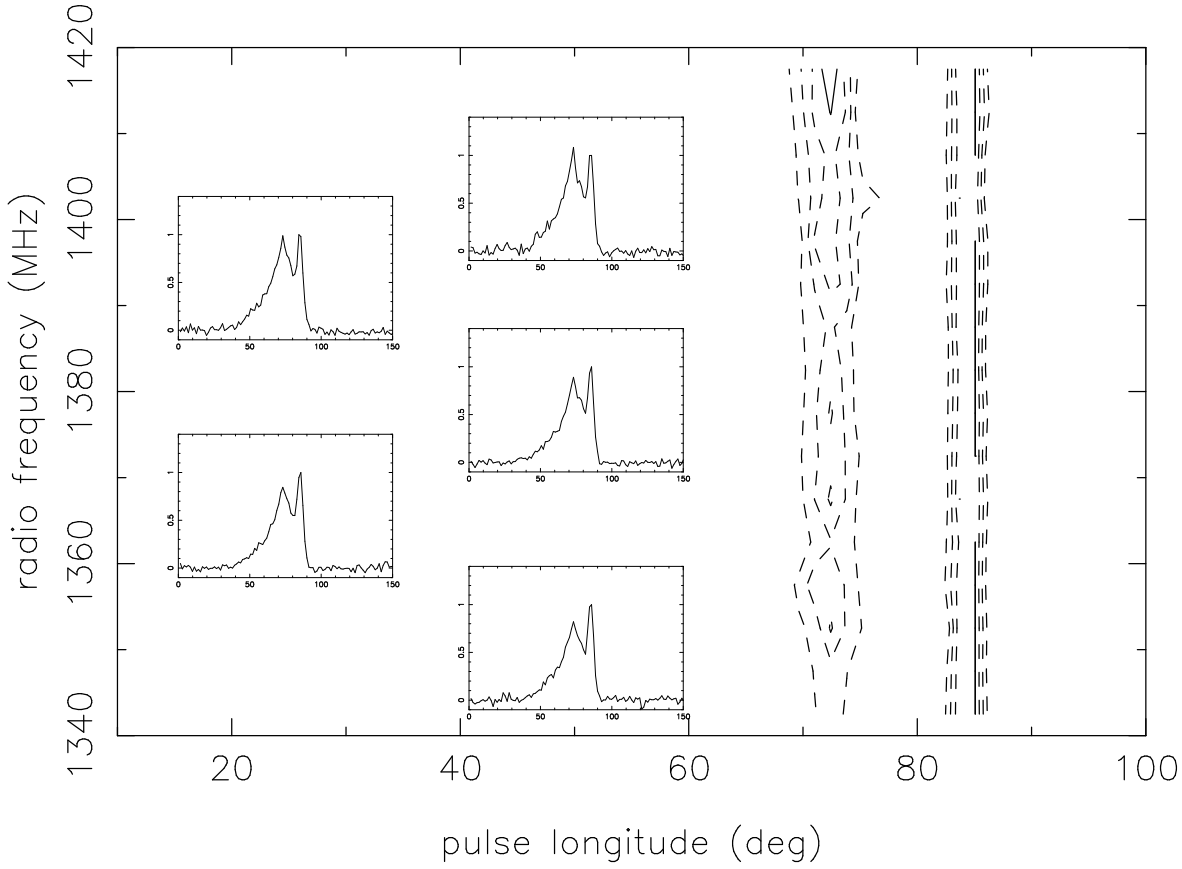

Fig. 3. Contour plot of pulse intensity as a function of pulse longitude and observing frequency for an average pulse profile constructed with 8 minutes of time series (approximately 30000 pulses) in all the 16 channels each of 5 MHz width. For clarity, height of the second component (h_2) has been normalised to unity in all the average pulse profiles (right-side vertical contour strip). The five inserts (from bottom to top) correspond to average profiles in channel numbers 1, 5, 9, 13 and 16. Contour level steps are in terms of root mean square error (see Eqn. 1). 'Solid' contour indicates the region where $h_1/h_2 \geq 1$. This figure has been plotted in the same style as Fig.8 in K99 for easier comparison.

be independent of interstellar scintillation effects and intrinsic to the pulsar magnetosphere.

4.2. Instabilities as a function of time

In order to study the profile changes as a function of time in more detail, we divided, as described above, our total observation time length into small segments of approximately 8 minutes in length, in each of the 16 frequency channels. With this set of profiles, normalized again to the trailing component, variations were also seen as a function of time. In Fig. 4 we show average profiles of these 8 minute segments stacked from bottom to top, in four different frequency channels (each of 5 MHz width). We also show the relative height of the first component with respect to the second (h_1/h_2), and the statistical significance of this value with respect to the minimum value of (h_1/h_2) in the data set ($= 0.77$) in square brackets. These significance values have been calculated with the error in the amplitude ratio, Δq, which is calculated as

$$\Delta q = \Delta h \sqrt{1+q^2} \approx \sqrt{2}\Delta h \quad (1)$$

where Δh is the error in component amplitude, taken to be one off-pulse RMS. From Fig. 4 it is clear that the observed profile variations are statistically significant.

Having shown that the profile variations occur both in time and narrow range of frequency, we now attempt to demonstrate the variation in both dimensions of the parameters simultaneously. Fig. 5 shows the gray scale (and contour) plot of this variation as a function of time (in X-axis) and radio frequency (in Y-axis). With a "pixel" size of 8 min×5 MHz, we again measure the ratio of the amplitudes of the leading and trailing components in each of the average profiles relative to its long-term average, and plot this number in a gray scale plot. The additionally drawn contours are chosen in steps of root mean square error, as computed again from Eqn. 1. The solid and dashed line contours indicate amplitudes of the leading component being larger or smaller than the amplitude of the long-term

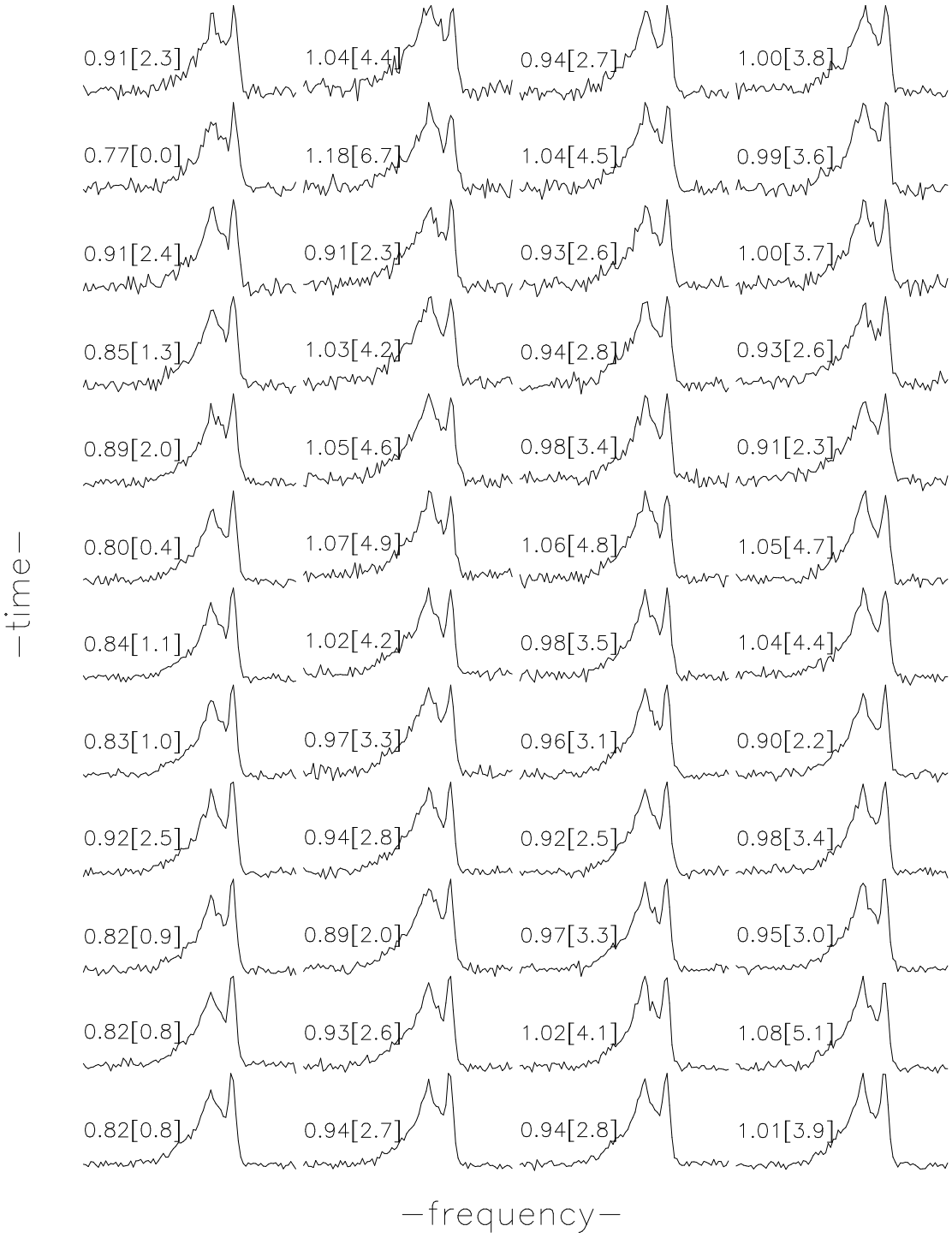

Fig. 4. Average pulse profiles as a function of time in four different frequency channels. Each average profile was created with 8 minutes of time series. The four columns correspond to frequency channels with centre frequencies of 1382.5, 1407.5, 1412.5 and 1417.5 MHz, respectively, with a channel width of 5 MHz. The fractional height of the first component (h_1/h_2) is also given for each profile, along with its deviation from the lowest ratio value (1^{st} column, 2^{nd} profile from top, ratio of 0.77) in terms of root mean square error (Eqn. 1). See text for details.

average, respectively. The two panels (top & bottom) of Fig.5 corresponds to our 1380 MHz and 840 MHz observations. As we can see in the top panel where the pulsar was bright, there are 6 contour levels, indicating that the fluctuations are statistically significant.

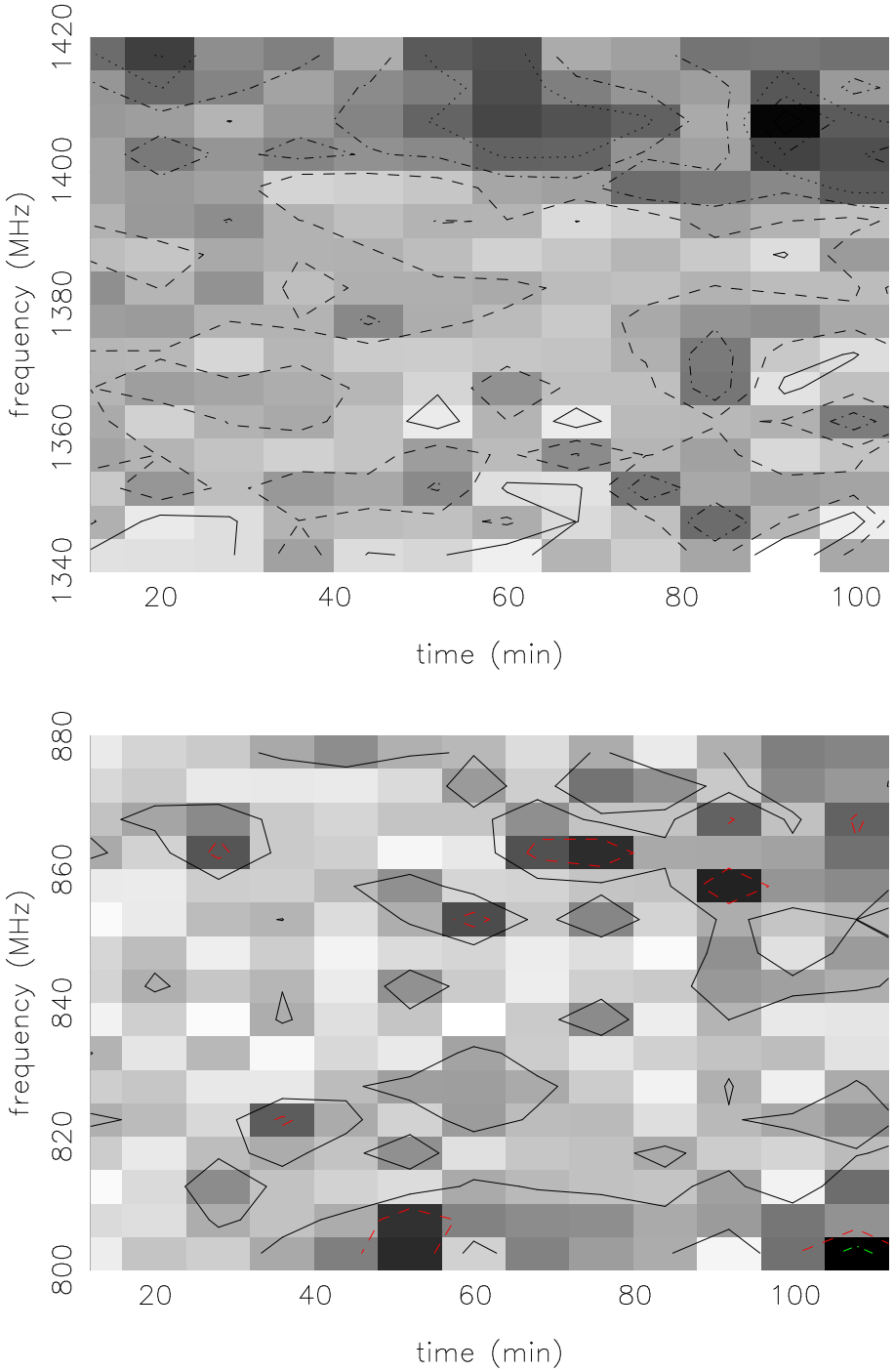

Fig. 5. Component amplitude ratio as a function of time (X-axis) and radio frequency (Y-axis). Each point corresponds to a time length of 8 min. Top panel corresponds to the observation at 1380 MHz, and the bottom panel to 840 MHz. Contour levels, in steps of root mean square error (see Eqn. 1), are indicated with different line styles for clarity. In the top panel, from the lowest contour level (white colour), the line style goes as 'solid', 'dash', 'dot-dash', 'dot-dot-dash', 'dotted', and 'solid'. The highest contour level corresponds to the darkest gray scale point. In the bottom panel, as the signal to noise ratio is not as high as that of the top panel, there are only three significant contour levels.

4.3. Time scales, frequency scales and the distribution of height ratios

Our previous analysis and that of K99 suggests the lack of a systematic trend in the variations as a function of time or frequency. In order to investigate in more detail as to whether there is a preferred quasi-periodicity or any preferred time or frequency scale, we computed histograms from observed changes in frequency and time. The results are summarised in Fig. 6. We computed these variations

by measuring the half-maximum points of the ratio variations along frequency and time axes in Fig. 5. That is, for the left panel in 6, frequency scale for each time pixel was measured, and for the right panel, time scale for each frequency channel was measured. It is clear that no clear tendency is observed. We also computed two-dimensional auto-correlation functions of the data shown in Fig. 5 with similar results.

Even though it is not possible to derive characteristic frequency or time scale, it is important to emphasize that the observed profile variations are highly significant. Both Fig. 4 & 5 show variations relative to high signal-to-noise templates which can be detected with high significance. Hence, the gray scale plots must not be mistaken for "noisy maps". The appearance is merely a different representation of the fact that typical time or frequency scales cannot be identified.

Having discussed the time scales and frequency scales, we also give in Fig. 7 the distribution of component height ratios. These component ratios were computed from the short-term 8 minute average profiles in each of the 5 MHz frequency channels. One of the possibilities for the observed profile variations is classical "mode-changing" (Backer 1970), which is well known among the normal pulsar population. Usually, if the mode-changing time scale is much shorter than the averaging time, averaging of several thousands of pulses is enough to get a stable profile even with the classical mode change. In the case of PSR J1022+1001, even after taking 8 minutes average (30,000 pulses), we still see variation. In order for mode-changing to have an effect on profile variation, then the time scale of these modes needs to be of the order of several minutes (less than 8 minutes).

As described by Kramer et al. (1999a), timing measurements obtained with the help of "adaptive" template (by gaussian component fitting method) gives the best timing residuals, and indicates that the variation that we see is much smoother than what one would expect from a strictly bimodal distribution. Nevertheless, from our data set alone we cannot rule out a case of classical mode-changing, e.g. where the strength of the primary mode dominates over a weaker, less probable secondary mode. However, the narrow-band profile variations as a function of frequency observed here and by Kramer et al. (1999a) cannot be explained by mode-changing.

5. Polarisation properties

In addition to the unusual instability in the pulse profile, PSR J1022+1001 has unusual polarisation properties. We have given in Fig. 8 the observed average linear polarisation position angle. This figure is a reproduction of Fig. 9 of K99 (refer to K99 for details on observing set-up.) In the top panel, we show the total intensity as well as the linearly and circularly polarised intensities. The PA curve is rather peculiar as it shows a step at about 35 deg longitude and a "notch" at about 50 deg longitude.

We have split the PA curve at the positions of the step and the notch into two separate parts, indicated by filled and open circles, respectively. Most remarkably, both resulting parts of the PA curve can be described by standard Radhakrishnan–Cooke (RC) models (Radhakrishnan & Cooke 1969) which only differ in their β value, i.e. angle of closest approach between the magnetic axis and the line of sight. Indeed, with $|\beta|$s of 1.5° and 4.5°, respectively, both RC models have the same α value (angle between the rotation and the magnetic axis) of 50° although this value is not very well constrained. The PA data intermediate between the two PA curves, indicated by "star" symbols, were ignored for the fit. An RC-model has also been fitted to PSR J1022+1001 by Xilouris et al. (1998) and Stairs et al. (1999), both attempting to fit the whole PA curve, but essentially ignoring most of the region designated by filled symbols in Fig. 8. Consistent with our results, at 1410 MHz Xilouris et al. (1998) derive values of $\alpha = 53.2°$ and $|\beta| = 7.3°$, while Stairs et al. (1999) obtain at 610 MHz $|\beta| = 4.9° \pm 1.8°$ and at 1410 MHz $|\beta| = 7.1° \pm 0.3°$.

One of the possible interpretations for this very interesting PA curve is to view these two parts as being caused by two polarisation emission modes (which may not be orthogonal) that arise from two different altitudes in the magnetosphere. In a cylindrical geometry, the inferred value of β (and α) for the two modes cannot be different, even if they are emitted from two different altitudes. However, as the emission altitudes of radio emission from MSPs are likely to be a good fraction of the light cylinder radius (Kramer et al. 1998), two effects may become important: aberration of the pulsar beam in a forward direction (i.e., earlier arrival times), and bending of the emission beam due to a sweep-back of the magnetic field lines near the light cylinder (i.e., later arrival times). Typically, aberration is the more prominent effect, in particular for fast rotating MSPs, unless the emission is originating from close to the light cylinder (e.g. Phillips 1992, Kramer et al. 1997). As the net result, if the emission corresponding to the two modes arises from two different altitudes, the derived values of β for the two modes could be different. The radiation associated with each component would then propagate through different parts of the pulsar magnetosphere. Depending on relative height and the different viewing geometries, described by the determined β-values, the leading component could hence be subject to (different) propagation effects which may then affect its apparent stability.

The intermediate PA-values ("star" symbols) could be explained by an incoherent addition of the two modes which are *not* orthogonal, as it has been observed for other pulsars before (e.g. McKinnon 2003). Curiously, this happens at longitudes which exactly coincide with the unstable leading component of the profile. We note that the idea that polarisation modes may be emitted from different heights is not new. McKinnon & Stinebring (1998; 2000) showed that the average pulse profiles corresponding to two orthogonal polarisation modes are different in their widths, indeed suggesting that modes are emitted at

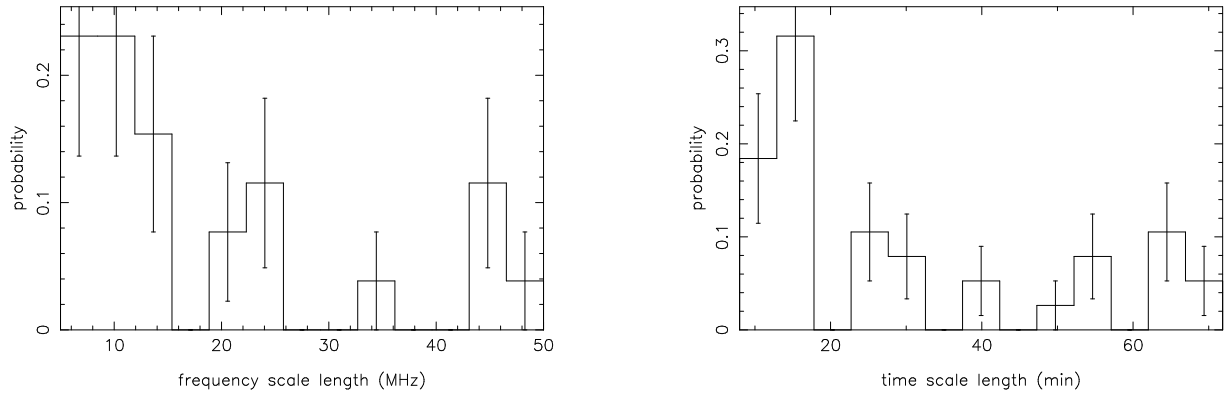

Fig. 6. Distribution of frequency and time scale lengths. Only the data set at 1380 MHz was used for this plot. As the plots show, a range of frequency and time scales are seen.

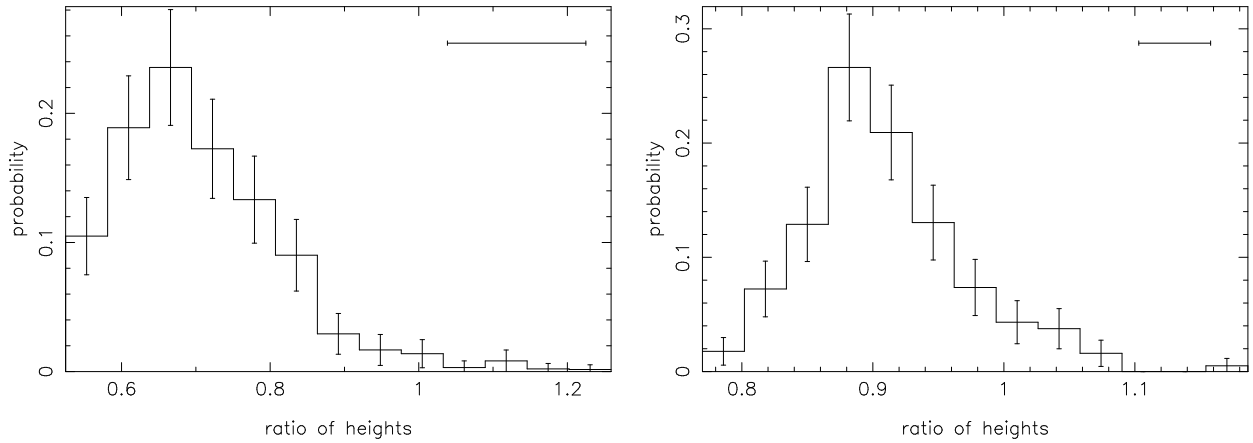

Fig. 7. Distribution of height ratios of the two components observed at 840 MHz (left) and 1380 MHz (right), for each 8 min. average profile in each 5 MHz frequency channel. Horizontal error bar in the top right corner indicates 1σ error. The total extent of the X-axis (from one extreme height ratio to the other) spans over several times the error bar, and hence the profile variations are statistically significant. See text for details.

separate altitudes. This effect has been further explored and modelled by Rankin & Ramachandran (2003) with a large sample of pulsars.

Another independent explanation for this peculiar PA behaviour, which may be more plausible, is derived from the work by Hibschman & Arons (2001). Following ideas first developed by Blaskiewicz et al. (1991), they examine the effect of aberration on the RC model curve, but also include polar cap current flows in their calculations. As they summarise, the current flow tends to shift the PA curve upwards (in Fig. 8), while aberration tends to shift the PA value in the opposite direction, causing also a phase shift of the whole PA curve. Most importantly, they also consider the possible effect of a return current in the pulsar magnetosphere. They argue that if our line-of-sight happens to penetrate a layer of this return current, this would appear as "jumps" in the PA curves at the corresponding pulse longitude values. In fact, Fig. 5 of Hibschman & Arons 2001 (reproduced here in Fig. 9) shows very remarkable similarity to our measured PA curve shown in Fig. 8. Their theoretical curve computed for an assumed set of parameters of $\alpha = 30$ deg, $\beta = 5$ deg and an emission height of 10% of the light cylinder radius, shows both a step as well as a notch, similar to what is actually observed for PSR J1022+1001.

Given this striking similarity between this theoretical prediction and our actual observed data, we are tempted to conclude that the discrete jumps that we see in the position angle are not related to orthogonal modes, but due to the return current layer as suggested by Hibschman & Arons (2001). If this is true, this is the first ever observational evidence for a return current in a pulsar magnetosphere.

The discrete jumps caused by the return current may be, as the authors indicate, frequency-dependent, depending on the nature of radius-to-frequency mapping, and the

total height of the emission region. Under these assumptions, in order derive definitive conclusions about the nature of the return current layer, one needs to study all the characteristics of the PA jumps, including their frequency dependence. We are currently undertaking such a detailed study, and the results will be presented in a following publication (Kramer, Ramachandran, Stairs & Athanasiadis, in prep.). Preliminary fits of the Hibschman & Arons model to our PA data suggest an emission height of 40% of the light cylinder radius and a current of about 75% of the Goldreich-Julian value, although further studies are needed to confirm these values.

As one can see, the unstable leading component in the pulse profile directly corresponds to the region bracketed by the discrete PA jumps at longitudes $\sim$ 35 deg and $\sim$ 50 deg (Fig. 8), which, in the above model, mark the longitudes of the return current layer. We propose here that the instability in the component strength is therefore due to the illuminated return current layer in the pulsar magnetosphere. Hibschman & Arons (2001) point out that although the return current layer is not normally thought of as a site of emission, it may be visible either through direct emission or through refraction or scattering of radiation of normal pulsar emission. While the physical reason for the instability of the component itself is not clear, the fact that the component appears at the same location as the discrete jump of the PA curve, and the similarity to the theoretical predictions of Hibschman & Arons (2001) may not be just a coincidence.

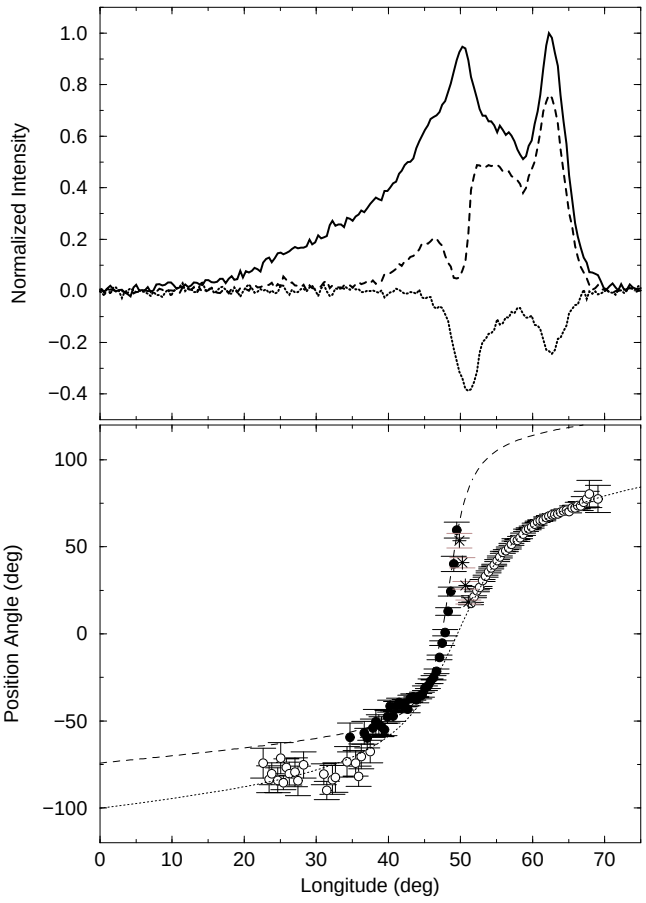

Fig. 8. Top panel gives the average pulse profile of PSR J1022+1001 at 1420 MHz (solid line), the average linearly polarised intensity (dashed line), and the average circularly polarised intensity (dotted line). The bottom panel shows the position angle of the linearly polarised emission component as a function of pulse longitude. See text for details.

6. Discussion and Conclusions

Our observations were conducted with the Westerbork Synthesis Radio Telescope (WSRT). In all our observing bands, WSRT has a dual-linear dipoles. The telescope is equatorially mounted, and hence the relative orientation of the direction of linear polarisation of the source remains the same, irrespective of the position of the source in the sky. This helps us in eliminating time-dependent profile variations due to possible residual cross-coupling effects. Moreover, as K99 showed (Fig. 9; see also Sallmen 1998 and Stairs et al. 1999), the degree of polarisation of the leading component is significantly less than that of the trailing component. If there is any spurious instrumental effect related to polarisation cross-coupling, we would expect more variations in the trailing component - in contrast to what we observe.

Therefore, without doubts we have confirmed the profile variations observed in PSR J1022+1001 as a function of time and, in particular, radio frequency. These variations are highly significant, as we have shown in Figs. 3 & 5. As for K99, this behaviour has been clearly observed in the 1340–1420 MHz band and is, for the first time, also clearly detected in at least another frequency band, i.e. 800–880 MHz. Due to signal-to-noise constraints, it was not possible to confirm these variations also with our 328 and 382-MHz frequency observations.

Even though Fig. 4 & 5 are reminiscent of an interstellar scintillation pattern, the relative variation of component amplitudes eliminates the possibility of a propagation effect outside the pulsar magnetosphere, as scintillation must affect both the components equally.

The observed profile changes does not seem to be consistent with *profile mode-change*, which is well known for the ordinary long period pulsar population. A smoothly distributed component ratios (Fig. 7) and their narrow band variations seem to rule out this possibility.

Lyutikov & Parikh (2000) and Lyutikov (2001) discuss the existence of a scattering and diffracting screen close to the light cylinder of fast rotating pulsars. While their estimates of the diffractive scales can vary within order of magnitude, they note that if the scattering is due to turbulence inside the pulsar magnetosphere it should be independent of frequency. Due to the apparent range of frequency scales suggested by Fig. 6 and 7, both at 840 and 1400 MHz, it is difficult to test this prediction, although

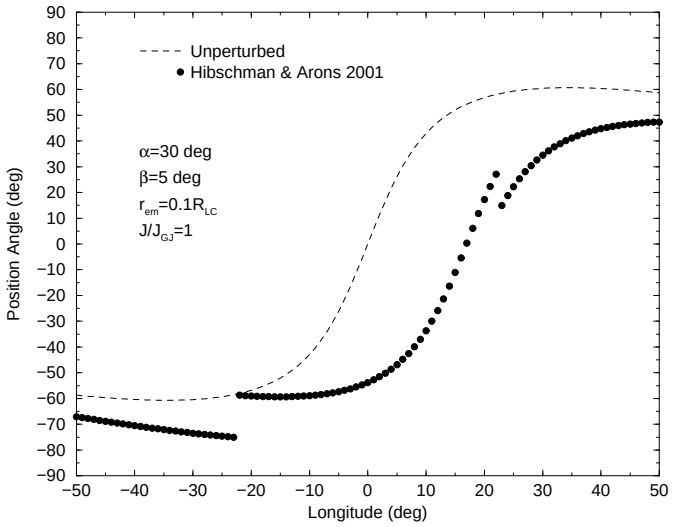

Fig. 9. Linear polarisation position angle as a function of pulse longitude. 'Dash' line shows the unperturbed curve, and the dotted line shows the curve after taking into account the effect of aberration and magnetospheric return currents. $r_{\rm em}$ & $R_{\rm LC}$ indicate emission height and light cylinder radius, respectively, and $(J/J_{\rm GJ})$ is the current in terms of Goldreich-Julian value. (reproduction of Fig. 5 of Hibschman & Arons 2001). The point with longitude value zero represents the closest approach of magnetic pole to the line of sight.

the profile variations shown in Fig. 6 appear similar at the first glance. However, the frequency scalings may be different for other types of scattering (Lyutikov, private communication) and it seems difficult to either confirm or reject the scattering screen model.

It is clear from Fig. 2 that the spectral properties of the unstable leading component are very different from that of the stable trailing component. Although the reason for this striking dissimilarity is unclear, it may well be related to the nature of the return current layer.

If our conclusions are correct, one would expect that this effect should also be visible for other pulsars. However, it is important to realize that for the involved aberration effect to become significant, relatively large emission heights are required, i.e. typically 10% of the light cylinder radius or more. For normal, slowly rotating pulsars, estimates for emission altitudes are usually much lower (e.g. Blaskiewicz et al. 1991, Phillips 1992, Kramer et al. 1997). However, for MSPs the emission appears to originate at larger fractions of the light cylinder radius (Kramer et al. 1998), so that these objects are indeed those where one would expect to observe the described effects at first. Indeed, a large fraction of MSPs is known to exhibit PA curves which are significantly different from what is expected for a classic RC curve (Xilouris et al. 1998, Stairs et al. 1999). A detailed study of MSP polarimetry data is part of the study currently underway (Kramer et al. in prep.)

7. Summary

With new multi-frequency data, we have demonstrated that the peculiar profile variations of PSR J1022+1001 over time and a narrow range of frequency can be observed at widely spaced radio frequencies. We propose two alternative models which are capable of explaining this interesting phenomenon. If the model currently favoured by the data is correct, our study would be the first ever observational evidence for a return current in a pulsar magnetosphere. If confirmed, future detailed studies will then allow measurements of basic properties of the plasma flow in the magnetosphere for the very first time.

Acknowledgements. We thank Jon Arons, D. C. Backer, A. G. Lyne, G. Smith and I. Stairs for all the discussions and critical comments. We also thank our referee, Simon Johnston, for his critical comments that have helped improve the manuscript.

References

Arzoumanian, Z. 1995, PhD-thesis, Princeton University
Backer, D. C., 1970, Nature, 228, 1297
Backer, D. C., & Sallmen, S. T., 1997, AJ, 114, 1539
Blaskiewicz M., Cordes J. M., & Wasserman I., 1991, ApJ, 370, 643
Camilo, F., 1994, PhD-thesis, Princeton University
Hankins, T. H., & Rickett, B. J. 1986, ApJ, 311, 684
Helfand, D. J., Manchester, R. N., & Taylor, J. H. 1975, ApJ, 198, 661
Helfand, D. J., Manchester, R. N., & Taylor, J. H., 1975, ApJ, 198, 661
Hibschman, J. A., & Arons, J., 2001, ApJ, 546, 382
Kramer, M., 1998, ApJ, 509, 856
Kramer, M., Wielebinski, R., Jessner, A., et al., 1994, A& AS, 107, 515
Kramer, M., Xilouris K. M., Jessner A., et al., 1997, A&A, 322, 846
Kramer, M., Xilouris K. M., Lorimer D.R., et al. 1998, ApJ, 501, 270
Kramer, M., Xilouris K. M., Camilo F., et al. 1999a, ApJ, 520, 324
Kramer, M., Lange Ch., Lorimer D. R., et al. 1999b, ApJ, 526, 957
Lyne, A.G., & Manchester, R.N., 1988, MNRAS, 234, 477
Lyutikov M., & Parikh A. 2000, in Proc. of IAU Colloq. 177, ASP Conf. Series Vol. 202, eds. M. Kramer, N. Wex & R. Wielebinski, pp. 393
Lyutikov M., 2001, Ap&SS, 278, 81
McKinnon, M. M., & Stinebring, D. R., 1998, ApJ, 502, 883
McKinnon, M. M., & Stinebring, D. R., 2000, ApJ, 529, 435
McKinnon, M., 2003, ApJ, in press
Mitra D. & Rankin J. M. 2002, ApJ, 577, 322
Moffett, D. A., & Hankins, T. H. 1996, ApJ, 468, 779
Phillips, J.A., 1992, ApJ, 385, 282
Radhakrishnan, V., & Cooke, D. J. 1969, Astrophys. Lett., 3, 225
Rankin, J. M. 1983, ApJ, 274, 333
Rankin, J. M., & Ramachandran, R., 2003, ApJ, 590, 411

Ruderman M. A., & Sutherland P. G., 1975, ApJ, 196, 51
Shitov, Yu.P., 1983, Sov. Astron., 27, 314
Sallmen S., 1998, Ph.D. Thesis, University of California at Berkeley
Stairs, I. H., Thorsett S.E., & Camilo F., 1999, ApJS, 123, 627
Stairs, I. H., et al., 2000, in IAU Colloq. 177, ASP Conference Series, eds. M. Kramer, N. Wex & R. Wielebinski, 202, 121
Taylor, J. H. 1994, in Les Prix Nobel, Norstedts Tryckeri, Stockholm, pp. 80-101
Weisberg, J. M., Romani, R. W., & Taylor, J. H., 1989, ApJ, 347, 1030
Xilouris, K. M., Kramer, M., Jessner, A., et al. 1998, ApJ, 501, 286